# A PARAMETRIC STUDY OF "WEAK LAYER" EFFECTS ON THE SEISMIC RESPONSE OF LIQUEFIABLE SOIL PROFILES

## Yannis Z. Tsiapas[1], Maria S. Spanea[1], and George D. Bouckovalas[1]

[1] National Technical University of Athens
Iroon Politexniou 9, 15780 Zografou, Attica, Greece
e-mail: ioannis.tsiapas@gmail.com, marspan53@gmail.com, gbouck@central.ntua.gr

**Abstract**

*The existence of a "weak" layer, of low relative density, within a liquefiable soil profile, may have a beneficial effect on the overall seismic response. The "weak" layer will liquefy earlier and may act as a "Natural Seismic Isolation" system, for the overlying, stronger, liquefiable layers, preventing thus the onset of liquefaction in them. In other words, it is possible that the liquefiable ground above the "weak" layer will not liquefy and may thus form a competent soil crust which will protect the integrity of infrastructure founded on it. The paper presents results of a parametric investigation of the "weak" layer effects on the overall seismic response of liquefiable soil profiles. It is based on nonlinear numerical analyses, performed with the Finite Difference method, and focuses on the effects of (i) soil properties (thickness and relative density) of the "weak" layer and the overlying liquefiable layers as well as (ii) the seismic motion characteristics on the extent of "weak" layer-induced natural seismic isolation.*

**Keywords:** Liquefaction, Numerical Analysis, Seismic Response, Natural Seismic Isolation.

## 1  INTRODUCTION

It is widely known that soil formations consisting of saturated, cohesionless soil layers are highly susceptible to earthquake induced excess pore pressure accumulation and liquefaction, with devastating results for infrastructures. However, it is possible that, under certain circumstances, the liquefaction of a soil layer prevents the propagation of seismic waves to the ground surface and leads to the drastic attenuation of seismic actions on infrastructures. Bouckovalas et al. [1] have shown that a uniform liquefiable layer, of adequate thickness and drastically reduced acoustic impedance, may indeed act as a "Natural Seismic Isolation" system for seismic ground motions.

The concept of "Natural Seismic Isolation" can be also generalized for non-uniform liquefiable layers which include an intermediate "weak" layer, with significantly degraded liquefaction resistance. In these soil profiles, the intermediate "weak" layer will liquefy first and will cause the attenuation of seismic motions, an effect which may prove beneficial for the overlying and more stiff sand layers. Hence, it will act as a "Natural Seismic Isolation" system, preventing liquefaction to extent up to the ground surface. In other words, the liquefiable ground above the "weak layer" will not liquefy and consequently it will maintain its strength and may thus act as a foundation bearing soil crust. To date, there are no research studies that systematically examine the above phenomena and suggest methods for their quantitative description. However, the few experimental and numerical studies that are found in the literature (e.g. [2,3]) confirm the abovementioned beneficial "weak" layer effect.

The scope of this paper is to investigate the seismic response and the liquefaction of non-uniform sand deposits, aiming to a qualitative evaluation of the "Natural Seismic Isolation" effect due to a "weak" soil layer embedded within the soil profile. For this purpose, a parametric investigation was performed focusing on the seismic response of non-uniform sand deposits. In total, approximately 100 nonlinear, fully coupled, one-dimensional effective stress numerical analyses aimed to examine the effect of various soil and seismic parameters on the seismic response of liquefiable sites with an intermediate "weak" layer.

## 2  NUMERICAL ANALYSES

All numerical analyses were conducted in the Finite Difference code FLAC [4], for the custom made soil profile depicted in Figure 1, which consists of five distinct soil layers under the groundwater table. The total thickness of the soil profile is $18\,m$, with the upper and the lower $2\,m$ consisting of non-liquefiable medium plasticity clay with plasticity index $PI=30$. The shear wave velocity of the clay crust and the clay bed layers is equal to $V_S=100$ and $300\,m/s$ respectively. The rest $14\,m$ consist of liquefiable sand of variable relative density $D_{r,o}$, with a "weak" layer of relative density $D_r=30\,\%$ and variable thickness $H_{weak}$ embedded in it.

The base of the soil column was shaken with a 15-cycle harmonic excitation, of peak acceleration $a_{max}=0.25\,g$ and variable period $T_{exc}$ (Figure 1). The values of: (i) the thickness of the "weak" layer $H_{weak}$, (ii) the total thickness of the overlying soil layers $H_{crust}$ (soil crust), (iii) the period of the seismic excitation $T_{exc}$ and (iv) the relative density $D_{r,o}$ of the stiffer sand layers were varied parametrically to cover a wide range site and earthquake conditions encountered in practice. The baseline analysis was conducted for the following reference values of the basic parameters: $H_{weak}=2\,m$, $H_{crust}=6\,m$, $D_{r,o}=60\,\%$ και $T_{exc}=0.3\,sec$.

The NTUA-SAND critical state plasticity constitutive model [5,6] was employed to simulate the response of the liquefiable sand, while the simpler Ramberg and Osgood [7] constitutive model was selected to simulate the nonlinear hysteretic response of clay layers. The NTUA-SAND model was calibrated against static and cyclic tests on saturated fine Nevada Sand [8], while the Ramberg and Osgood [7] model was calibrated against the experimental

modulus reduction and damping curves of Vucetic and Dobry [9] for low plasticity ($PI=30$) clays. Free-field lateral boundaries were simulated with the "tied-node" technique, which imposes the same (horizontal and vertical) boundary displacements at grid-points of the same elevation. The "Selective Filtering Method" [10] was used in order to eliminate the numerical noise which is inherent to elastoplastic dynamic analyses with FLAC, while the overall accuracy of the numerical methodology has been successfully evaluated in similar studies in the past [e.g. 11,12].
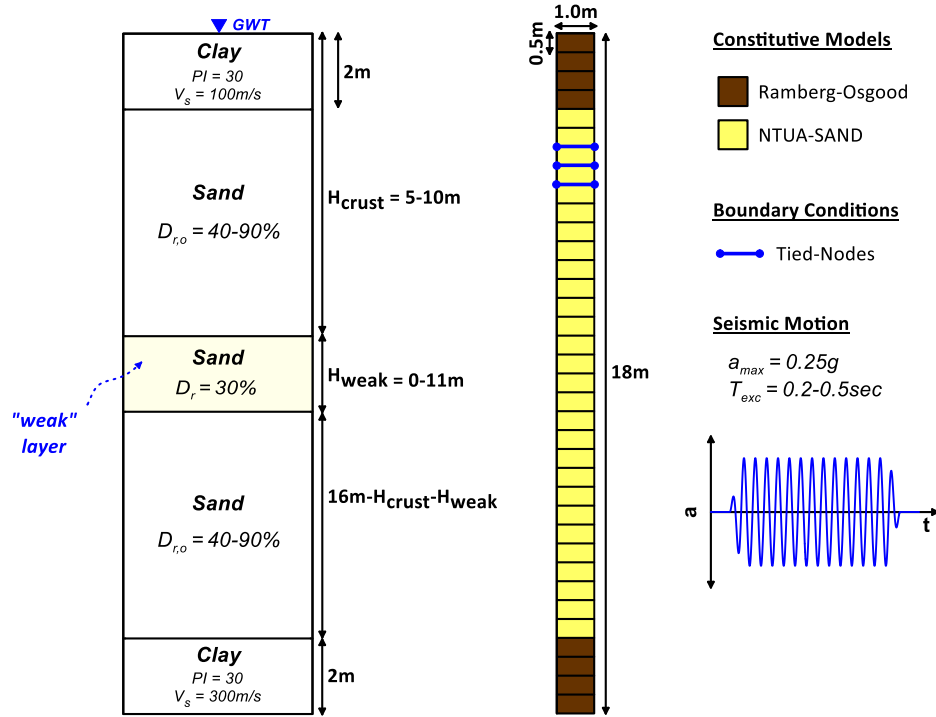


Figure 1: Soil profile, Finite Different mesh and input motion oF the numerical simulations.

## 3   MECHANISMS OF WEAK LAYER EFFECT

To identify the mechanisms which control "weak" layer effects, and demonstrate their consequences on the seismic response of non-uniform sand deposits, the results of a typical analysis with $H_{weak}=2\,m$, $H_{crust}=8\,m$, $D_{r,o}=60\,\%$ and $T_{exc}=0.3\,sec$ are first presented in more detail. For comparison purposes, the numerical analysis was repeated for the case of uniform sand of relative density $D_{r,o}=60\,\%$ over the entire $2$-$16\,m$ depth, namely without intermediate "weak" layer (i.e. $H_{weak}=0\,m$). Figures 2a and 2b compare the time-histories of the excess pore pressure ratio $r_u$, defined as the ratio of the excess pore pressures $\varDelta u$ over the initial effective vertical stress $\sigma'_{v,o}$ (i.e. $r_u=\varDelta u/\sigma'_{v,o}$), in the middle of the top sand layer as well as in the middle of the "weak" layer, for the cases of uniform and non-uniform sand respectively. In addition, Figures 2c and 2d present the respective comparisons for the time-histories of the shear stress ratio $CSR=\tau_d/\sigma'_{v,o}$ (where $\tau_d$ is the seismic shear stress amplitude).

As depicted by the $r_u$ time-histories of the non-uniform ground (Figures 2a and 2b), liquefaction occurs first in the "weak" layer at approximately $t=0.8\,sec$, and affects significantly the evolution of the excess pore pressures on the sandy layers above and below the "weak" one. Following the red lines in Figures 2a and 2b, it is observed that after the time instance $t=0.8\,sec$, the excess pore pressure ratio in the "weak" layer becomes almost unity ($r_u\approx0.8$-$1.0$) practically diminishing the shearing resistance of that layer. The result of this is to decelerate the excess pore pressure buildup in the overlying layer of relative density $D_{r,o}=60\,\%$ and

prevent the onset of liquefaction that would have occurred in the absence of the "weak" layer (black line). The above observations are in total accordance with the respective *CSR* time-histories in Figures 2c and 2d, where it is observed that around $t = 1.0$ sec the amplitude of the $\tau_d / \sigma'_{v,o}$ ratio above the "weak" layer drops to significantly lower levels. This observation, in combination with the small excess pore pressure ratios at these depths, leads to the conclusion that the liquefaction of the "weak" layer actually functions as a "Natural Seismic Isolation" system for the overlying sand layer.
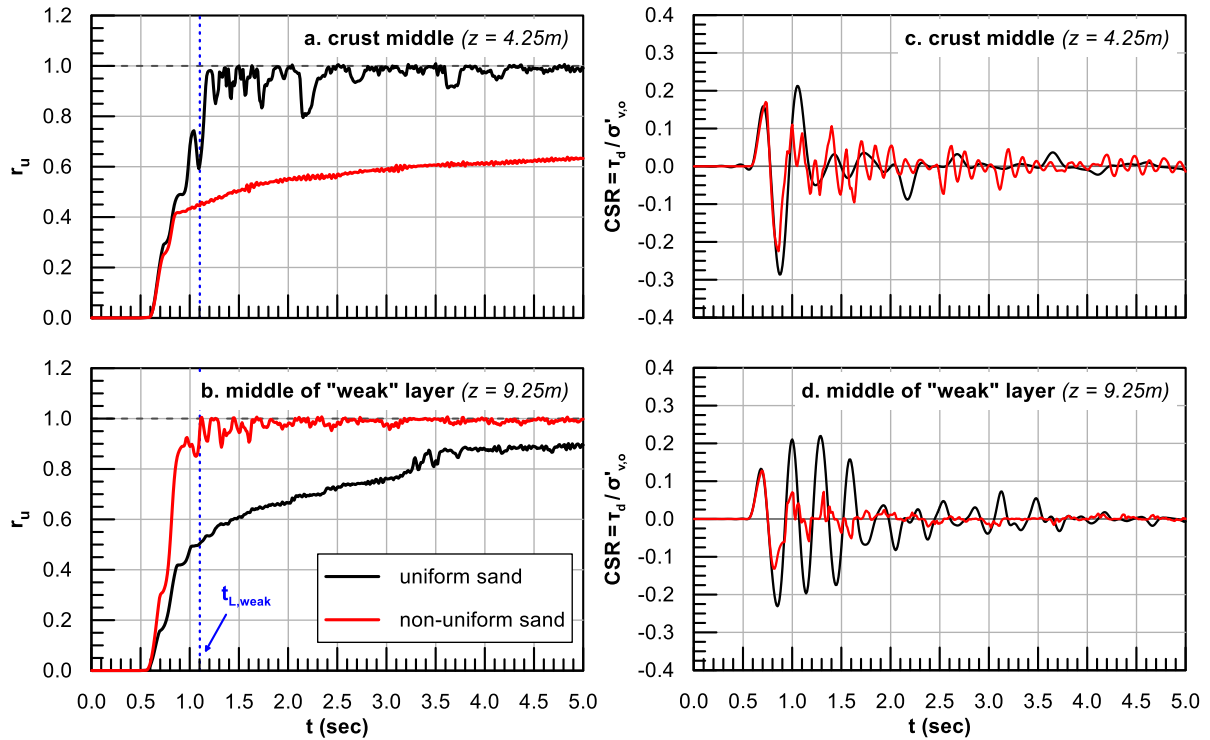


Figure 2: Typical time histories of excess pore pressure ratio $r_u$ and shear stress ratio *CSR* at the middle of the "weak" layer and the overlying layer of sand.

For further insight, Figure 3a compares the variation with depth of the maximum excess pore pressure ratio $r_{u,max}$ for both the non-uniform and the uniform soil profiles. It is observed that due to the existence of the "weak" layer, liquefaction has not occurred at any depth in the sand layer above it. In particular, the average value of the maximum excess pore pressure ratio above the "weak" layer $r_u^{cr}$ has been reduced from $r_u^{cr} \approx 1.0$ for the uniform sand deposit to the value $r_u^{cr} = 0.65$ in the presence of the "weak" layer. It is also observed that the effect of the "weak" layer is also beneficial on the seismic response of the liquefiable sand layer below it, although less significant and consistent than for the overlying sand layer. For this reason, the following presentation will focus only upon results for the overlying sand layer.

The variation of the factor of safety against liquefaction $FS_L$ with depth is depicted in Figures 3b and 3c for the case of non-uniform and uniform sand deposit respectively. In both cases, the values of the factor of safety were estimated following two different approaches. Initially, $FS_L$ was estimated via the empirical methodologies that are commonly utilized in practice (e.g. [13]), based on the results of in-situ SPT or CPT tests. More specifically, it was assumed that the number of SPT blow counts is equal to $N_{1,60} = 4.1$ and 16.5 for $D_r = 30\%$ and $D_{r,o} = 60\%$ respectively [14]. For the estimation of the seismic actions, the nonlinear numerical analyses were repeated under drained conditions, i.e. without excess pore pressures

buildup and liquefaction onset. In parallel, the values of $FS_L$ which correspond to the actual response of each soil element during the numerical simulation were estimated, as follows:

$$FS_L = \left( \frac{N}{N_L} \right)^{-b} \tag{1}$$

where $N$ is the applied number of cycles by the seismic motion and $N_L$ the number of loading cycles required to cause liquefaction based on the numerical analysis results. Equation (1) is based on the mathematical expression of the liquefaction resistance curve, namely on the correlation between the cyclic stress ratio $CSR$ and $N_L$:

$$CSR = a \cdot N_L^{-b} \tag{2}$$

where the values of coefficient $a$ and of exponent $b$ depend on soil type and loading conditions. For the NTUA-SAND constitutive model and for Nevada Sand, it was assumed that $b = 0.41 - 0.57$, based on the previous work of Kalogeraki and Zontanou [15]. More information regarding the estimation of $FS_L$ from the numerical analysis results can be found in [15-17].
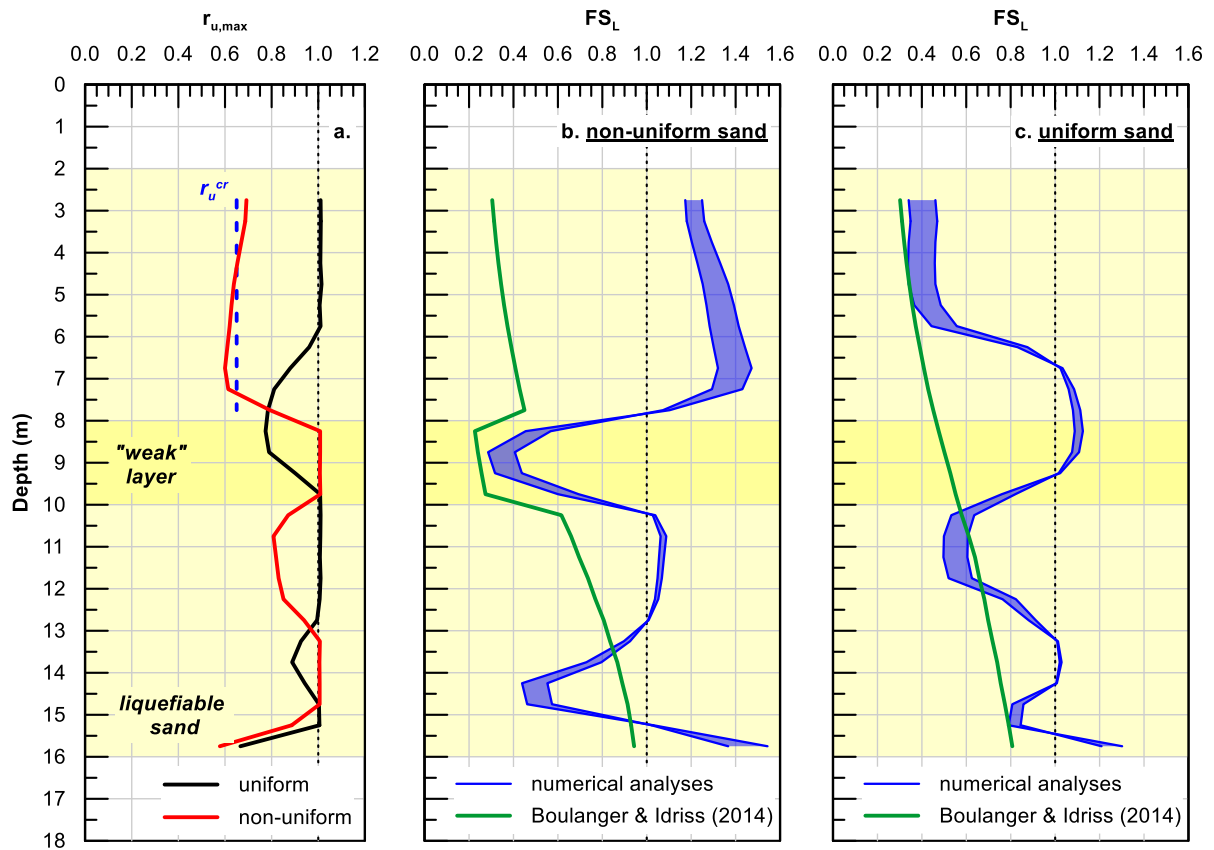


Figure 3: Typical variation with depth of (a) maximum excess pore pressure ratio $r_{u,max}$ and $FS_L$ considering (b) non-uniform and (c) uniform sand deposit.

According to Figure 3b, the values of the factor of safety against liquefaction on the top sand layer, based on the numerical analysis results and Eq (1), vary in the range $FS_L = 1.15 - 1.45$, compared to the considerably smaller $FS_L$ values ($FS_L = 0.30 - 0.45$) which were computed for the "weak" layer. It is thus evident that due to the onset of liquefaction in the "weak" layer, the applied shear stress ratio $CSR$ in more shallow depth is reduced, acting thus benefi-

cially for the overlying sand layers, which have not been already liquefied. As the applied seismic action is reduced, the factor of safety against liquefaction at these depths increases significantly to values larger than unity, implying that the onset of liquefaction has been prevented. On the contrary, it is shown that the empirical methodologies that are used in practice, which cannot take into account the presence of the "weak" layer, are entirely misleading as they predict that the top sand layer will also liquefy and exhibit $FS_L \approx 0.30\text{-}0.40$. For the "weak" layer, where the onset of liquefaction actually occurs, the two methodologies give compatible results.

Similar conclusions arise even in the case of a uniform sand deposit (Figure 3c). In particular, the empirical methodologies give compatible results with the numerical analyses only for the depths that liquefy first, while they predict considerably smaller $FS_L$ values in all other depths. This means that the empirical methodologies for the estimation of $FS_L$, which are based on in-situ test results, are valid with acceptable accuracy only for the depths which correspond to the minimum factor of safety against liquefaction $FS_{L,min}$, as they do not take into account the drastic attenuation of the seismic actions in the soil deposits above the depth where liquefaction is first triggered (or equivalently the minimum $FS_L$ value).

## 4 PARAMETRIC INVESTIGATION

In total, about 100 numerical analyses were performed, to explore the effect of the following basic parameters: *(i)* the thickness of the "weak" layer $H_{weak}$ ($=0\text{-}11$ m, at 1 m increments), *(ii)* the thickness of the top sand layer $H_{crust}$ ($=5\text{-}10$ m, at 1 m increments), *(iii)* the excitation period $T_{exc}$ ($=0.2\text{-}0.5$ sec, at 0.1 sec increments) and, finally, *(iv)* the relative density of the stiffer sand layers $D_{r,o}$ ($=40\text{-}90\%$ at 10 % increments).

Initially, the analysis of Section 3 was repeated for values of the "weak layer" thickness varying in the range $H_{weak}=0\text{-}8$ m, while its top remained constant at $z=8$ m (namely with constant $H_{crust}=8$ m). Figure 4a depicts the variation of the average value (with depth) of the maximum excess pore pressure ratio in the top liquefiable sand layer $r_u^{cr}$ with the thickness of the "weak" layer $H_{weak}$. In the same figure, the total range of $r_{u,max}$ values in the liquefiable zones of the top sand layer is also presented. It is observed that the thickness of the "weak" layer $H_{weak}$ is a basic parameter as it significantly affects the value of $r_u^{cr}$. It is noteworthy that even a very thin liquefiable "weak" layer with $H_{weak}=1$ m can prevent the onset of liquefaction on the overlying sand layers. In addition, it is observed that for larger $H_{weak}$ thickness values the $r_u^{cr}$ diagrams tend to stabilize to a minimum value $min(r_u^{cr})$, which denotes the maximum possible reduction of excess pore pressures in the top sand layer, or else the maximum possible "Natural Seismic Isolation" that can be achieved. In the examined case, the increase of the thickness of the "weak" layer $H_{weak}$ leads to a significant reduction on $r_u^{cr}$ values until the minimum value $min(r_u^{cr})=0.49$ is reached, which corresponds to the numerical analyses with thickness equal to $H_{weak}=8$ m.

The format of Figure 4a was adopted for the presentation of the effect of all examined parameters in the present numerical investigation (i.e. $H_{crust}$, $T_{exc}$, $D_{r,o}$). In particular, the diagrams of the $r_u^{cr}$ variation with the thickness of the "weak" layer $H_{weak}$ are depicted in Figure 4b for different top sand layer thicknesses $H_{crust}$, in Figure 4c for different excitation periods $T_{exc}$ and in Figure 4d for different values of the relative density $D_{r,o}$ of the stiffer sand layers. Figure 4b shows that not only the shape of the $r_u^{cr}\text{-}H_{weak}$ diagrams but also the minimum values $min(r_u^{cr})$ are similar in all numerical analyses with different thickness of the top sand layer $H_{crust}$. In other words, the thickness of the top sand layer, namely the depth where the "weak" layer is met, does not seem to have a significant effect on the values of $r_u^{cr}$.

On the other hand, Figure 4c shows that the shape of the diagram alters significantly based on the period $T_{exc}$ of the seismic excitation. In particular, it is observed that the excitation pe-

riod has no effect on the values of the minimum $r_u^{cr}$ ratio $min(r_u^{cr})$, which in all cases is approximately equal to $min(r_u^{cr}) \approx 0.50$, but affects the reduction rate of $r_u^{cr}$ with $H_{weak}$, which decreases as the excitation period increases. This effect becomes more prominent for $T_{exc} = 0.5$ sec. This practically means that for larger $T_{exc}$ periods the $H_{weak}$ thickness that is required in order to achieve the maximum possible reduction in the mean pore pressure ratio of the top sand layer increases. In more detail, for $T_{exc} = 0.2$ sec the minimum ratio $min(r_u^{cr})$ is achieved for $H_{weak} = 3$ m, while for $T_{exc} = 0.5$ sec it is achieved for $H_{weak} = 10$ m. It should be noted that this observation is in accordance with the findings of Bouckovalas et al. [1], who showed that the excitation period is one of the basic parameters which affect the minimum thickness of liquefied sand that is required for drastic attenuation of the seismic actions on the ground surface.
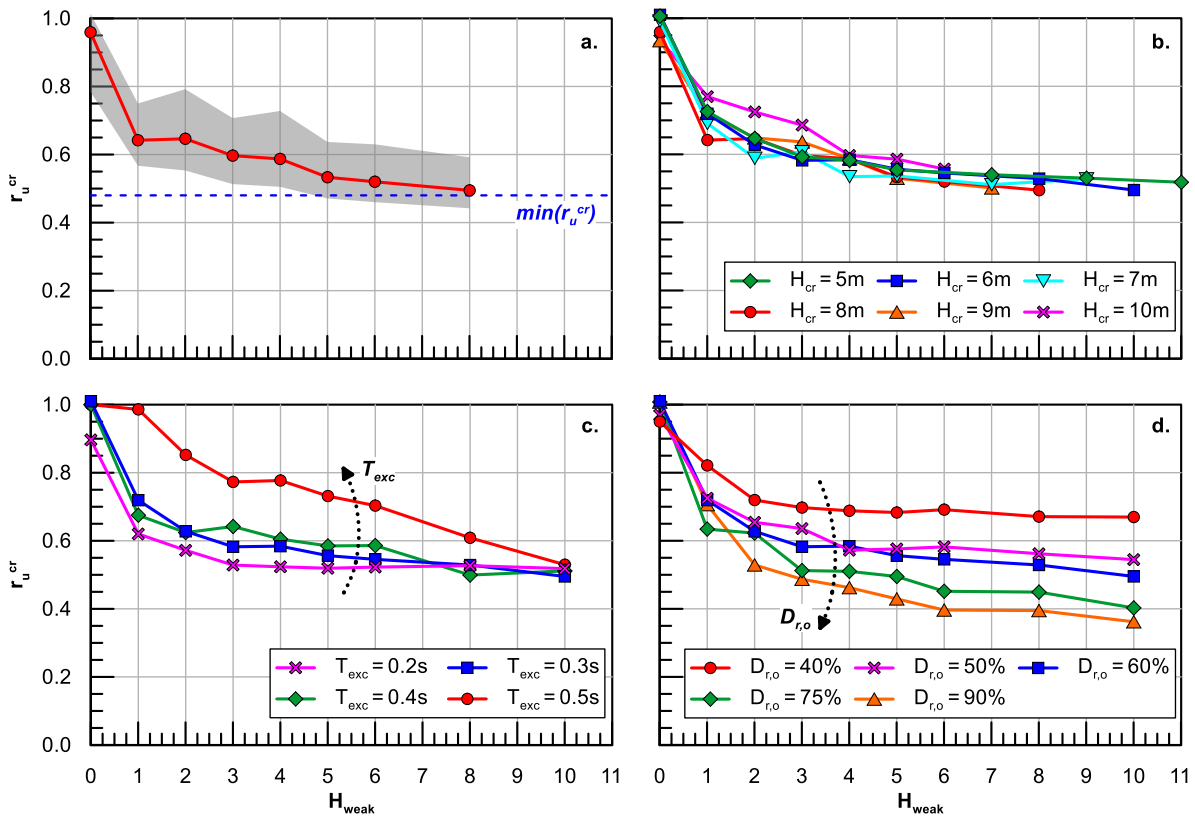


Figure 4: Effect of parameters: (a) $H_{weak}$, (b) $H_{cr}$, (c) $T_{exc}$ and (d) $D_{r,o}$ on the variation of the average pore pressure ratio in the top sand layer $r_u^{cr}$.

Finally, Figure 4d shows that the relative density $D_{r,o}$ of the stiffer sand layers constitutes also a crucial parameter for the definition of the minimum $r_u^{cr}$ value $min(r_u^{cr})$, which reduces significantly with the increase of $D_{r,o}$. Apart from that, the shape of $r_u^{cr}$-$H_{weak}$ diagrams is similar for all different relative densities $D_{r,o}$. It is worth mentioning that even for relative density $D_{r,o} = 40\%$, i.e. slightly larger than that of the "weak" layer ($D_r = 30\%$), a reduction in the values of $r_u^{cr}$ is observed, which implies that even a small difference in the soil conditions of the "weak" layer, relative to the rest liquefiable ground, is adequate in order to achieve "Natural Seismic Isolation" conditions.

For a more detailed insight in the effect of the relative density of the stiffer layer $D_{r,o}$ on the values of the minimum ratio $min(r_u^{cr})$, Figure 5 shows the variation of $min(r_u^{cr})$ values with the relative density of the top sand layer $D_{r,o}$. It is thus observed that the minimum value of

$r_u^{cr}$ reduced from $min(r_u^{cr}) \approx 0.67$ for relative density $D_{r,o} = 40\%$ to $min(r_u^{cr}) \approx 0.36$ for $D_{r,o} = 90\%$, while the reduction rate of $min(r_u^{cr})$ reduces with the increase of $D_{r,o}$ value.
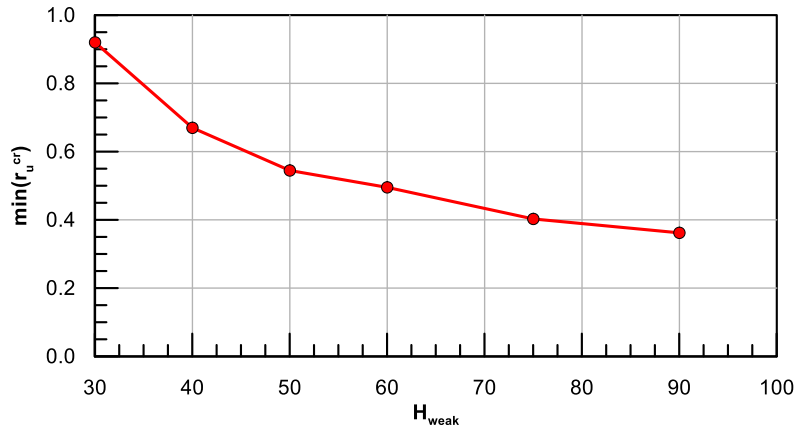


Figure 5: Variation of $min(r_u^{cr})$ with the relative density of the top sand layer $D_{r,o}$.

## 5  CONCLUSIONS

In the present study, the seismic response of non-uniform liquefiable sand deposits with an embedded "weak" sand layer of low relative density and significantly downgraded liquefaction resistance is examined. In such deposits, the "weak" layer liquefies earlier than the stiffer sand layers above and below it and forms a "Natural Seismic Isolation" system for the stiffer overlying layers, which are now protected and maintain low excess pore pressure ratio values, in the order of $r_u = 0.40 - 0.70$. The "weak" layer effect on the seismic response of the underlying liquefiable layer is also beneficial, but not as important and consistent as for the overlying layer.

The parametric analyses of this study revealed that the average values of the maximum excess pore pressure ratio that develop in the overlying sand layer $r_u^{cr}$ depend on the following site and seismic excitation parameters: *(i)* the thickness of the "weak" layer $H_{weak}$, *(ii)* the excitation period $T_{exc}$ and *(iii)* the relative density $D_{r,o}$ of the stiffer layers. In particular, the increase of the thickness $H_{weak}$ leads to reduction of $r_u^{cr}$ values until a minimum value ($0 < min(r_u^{cr}) < 1$), the increase of the excitation period $T_{exc}$ reduces the reduction rate of $r_u^{cr}$ with the increase of $H_{weak}$, without however affecting the aforementioned $min(r_u^{cr})$ value, while the increase of $D_{r,o}$ leads to a reduction of the $min(r_u^{cr})$ values. Finally, the depth of the "weak" layer surface ($H_{crust}$) has no substantial effect on the seismic system response.

Furthermore, it has been shown that the empirical methodologies which are widely applied in practice for the estimation of $FS_L$ based on in-situ test results (e.g. [13]) can be applied with satisfactory accuracy only for the depths corresponding to the minimum factor of safety against liquefaction $FS_{L,min}$, while they significantly underestimate the actual value of $FS_L$ mainly for shallower depths.

It should be finally noted that the present research is currently in progress, aiming to study the effect of additional parameters, such as the relative density of the "weak" layer and the permeability of the liquefiable sand, as well as to propose an analytical methodology for the prediction of the average value (with depth) of the maximum excess pore pressure ratio $r_u^{cr}$ and of the factor of safety against liquefaction in the top sand layers.

## 6  ACKNOWLEDGEMENTS

## REFERENCES

[1] G.D. Bouckovalas, Y.Z. Tsiapas, A.I. Theocharis, Y.K. Chaloulos, Ground response at liquefied sites: seismic isolation or amplification? *Soil Dynamics and Earthquake Engineering*, 91, 329-339, 2016.

[2] L. Gonzalez, T. Abdoun, M.K. Sharp, Modeling of seismically induced liquefaction under high confining stress. *International Journal of Physical Modeling in Geotechnics*, 2(3), 1–15, 2002.

[3] M. Taiebat, B. Jeremić, Y.F. Dafalias, A.M. Kaynia, Z. Cheng, Propagation of seismic waves through liquefied soils. *Soil Dynamics and Earthquake Engineering*, 30(4), 236-257, 2010.

[4] Itasca, *FLAC version 7.0*. Itasca Consulting Group Inc, 2011.

[5] A.G. Papadimitriou, G.D. Bouckovalas, Plasticity model for sand under small and large cyclic strains: A multiaxial formulation. *Soil Dynamics and Earthquake Engineering*, 22(3), 191-204, 2002.

[6] K.I. Andrianopoulos, A.G. Papadimitriou, G.D. Bouckovalas, Bounding surface plasticity model for the seismic liquefaction analysis of geostructures. *Soil Dynamics and Earthquake Engineering*, 30(10), 895-911, 2010.

[7] W. Ramberg, W.R. Osgood, *Description of stress-strain curve by three parameters*. Technical note 902, National Advisory Committee for Aeronautics, 1943.

[8] K. Arulmoli, K.K. Muraleetharan, M.M. Hossain, L.S. Fruth, *VELACS: verification of liquefaction analyses by centrifuge studies; Laboratory Testing Program – Soil Data Report*. Research Report, The Earth. Technology Corporation, 1992.

[9] M. Vucetic, R. Dobry, Effect of soil plasticity on cyclic response. J*ournal of Geotechnical Engineering*, 117(1), 89-107, 1991.

[10] Y.Z. Tsiapas, G.D. Bouckovalas, Selective Filtering of Numerical Noise in Liquefiable Site Response Analyses. *Geotechnical Special Publication, GSP 292,* 248–257, 2018.

[11] G.D. Bouckovalas, Y.Z. Tsiapas, V.A. Zontanou, C.G. Kalogeraki, Equivalent Linear Computation of Response Spectra for Liquefiable Sites: The spectral envelope method. *Journal of Geotechnical and Geoenvironmental Engineering,* 143(4), 4016115, 2017.

[12] Y.Z. Tsiapas, G.D. Bouckovalas, Equivalent linear computation of response spectra for liquefiable sites: The spectral interpolation method. *Soil Dynamics and Earthquake Engineering*, 116, 541-551, 2019.

[13] R.W. Boulanger, I.M. Idriss, *CPT and SPT based liquefaction triggering procedures*. Report No. UCD/CGM-14/01, Center for Geotechnical Modeling, U.C. Davis, 2014.

[14] I.M Idriss, R.W. Boulanger, *Soil Liquefaction During Earthquakes*. Earthquake Engineering Research Institute, Oakland, California, USA, 2008.

[15] C.G. Kalogeraki, V.A. Zontanou, *Re-evalution of factor of safety against seismic liquefaction*." Diploma Thesis, NTUA, Athens, 2014.

[16] Y.Z. Tsiapas, *Seismic Response Analysis of Liquefiable Ground with Computational Methods.* PhD Thesis, Department of Civil Engineering, NTUA, Athens, 2017.

[17] M.S. Spanea, *Evolution of Earthquake-induced Liquefaction on Sand Deposits with Intermediate "Weak" Layer.* Diploma Thesis, NTUA, Athens, 2019.